

Intermolecular Cross-linking between the Periplasmic Loop_{3–4} Regions of PomA, a Component of the Na⁺-driven Flagellar Motor of *Vibrio alginolyticus**‡

Received for publication, February 3, 2000, and in revised form, July 17, 2000
Published, JBC Papers in Press, July 18, 2000, DOI 10.1074/jbc.M000848200

Tomohiro Yorimitsu, Yukako Asai, Ken Sato, and Michio Homma‡

From the Division of Biological Science, Graduate School of Science, Nagoya University, Chikusa-Ku, Nagoya 464-8602, Japan

PomA and PomB form a complex that conducts sodium ions and generates the torque for the Na⁺-driven polar flagellar motor of *Vibrio alginolyticus*. PomA has four transmembrane segments. One periplasmic loop (loop_{1–2}) connects segments 1 and 2, and another (loop_{3–4}), in which cysteine-scanning mutagenesis had been carried out, connects segments 3 and 4. When PomA with an introduced Cys residue (Cys-PomA) in the C-terminal periplasmic loop (loop_{3–4}) was examined without exposure to a reducing reagent, a 43-kDa band was observed, whereas only a 25-kDa band, which corresponds to monomeric PomA, was observed under reducing conditions. The intensity of the 43-kDa band was enhanced in most mutants by the oxidizing reagent CuCl₂. The 43-kDa band was strongest in the P172C mutant. The motility of the P172C mutant was severely reduced, and P172C showed a dominant-negative effect, whereas substitution of Pro with Ala, Ile, or Ser at this position did not affect motility. In the presence of DTT, the ability to swim was partially restored, and the amount of 43-kDa protein was reduced. These results suggest that the disulfide cross-link disturbs the function of PomA. When the mutated Cys residue was modified with *N*-ethylmaleimide, only the 25-kDa PomA band was labeled, demonstrating that the 43-kDa form is a cross-linked homodimer and suggesting that the loops_{3–4} of adjacent subunits of PomA are close to each other in the assembled motor. We propose that this loop region is important for dimer formation and motor function.

Many bacteria rotate flagellar filaments to swim. The flagellar filament is attached via a flexible hook to a protein complex termed the basal body, which is embedded in the cell surface. The motor is composed of the basal body and the C ring (rotor), whereas the multiple torque-generating units of the stator surround the rotor (1). The motor is driven by the flow of specific ions (H⁺ or Na⁺) through the stator, and mechanical force is presumably generated at the stator-rotor interface (2, 3).

Escherichia coli has H⁺-driven flagellar motors whose torque-generating units consist of two proteins, MotA and MotB. These two proteins are believed to form a H⁺ channel to permit the H⁺ influx and to provide the energy for motor rotation

(4–7). In contrast, the polar flagellum of *Vibrio* spp., *Vibrio alginolyticus*, *Vibrio parahaemolyticus*, and *Vibrio cholerae* is driven by the Na⁺-motive force, and the products of four genes, *pomA*, *pomB*, *motX*, and *motY*, are essential for Na⁺-driven rotation (8–15). Of these, PomA and PomB are similar to MotA and MotB, respectively. It has been inferred that PomA and PomB also form an ion channel (8). This inference was supported by the observation that mutations conferring resistance to phenamil, which is a known Na⁺-channel inhibitor and specifically and strongly inhibits the Na⁺-driven motor, mapped to *pomA* and *pomB* (14, 16, 17). The mutations occurred at Asp-148 of PomA and Pro-16 of PomB, which are near the cytoplasmic ends of putative transmembrane segments. The D148Y and P16S mutations combined to produce a synergistic increase in resistance to phenamil and impaired motor function much more severely than the individual mutations in the absence of inhibitor (17). We have also shown that PomA and PomB physically interact with each other (18), and that Na⁺ influx can be detected in reconstituted proteoliposomes containing purified PomA/PomB complex (19). The molar ratio of the isolated complex is calculated to be 2PomA/1PomB, and PomA seems to form a stable dimer.

To characterize the molecular architecture of PomA, we carried out Cys-scanning mutagenesis (20). This technique is useful for determining the structure and function of many proteins (21–24). In PomA, periplasmic loops are predicted for residues Val-21 through Leu-36 between transmembrane segments 1 and 2 (loop_{1–2}) and for residues Ser-167 through Ala-180 between transmembrane segments 3 and 4 (loop_{3–4}) (Fig. 1). Each residue in these loops has been substituted with Cys. Except for A174C, all Cys substitutions from M169C to M179C in loop_{3–4} impaired motility, whereas only the D31C substitutions in loop_{1–2} significantly impaired motility. The motility of some Cys mutants was inhibited by the thiol-modifying reagents 5,5'-dithiobis(nitrobenzoic acid) and NEM.¹ The inhibition profiles of these reagents were consistent with the membrane topology predicted from the hydrophobicity profiles (20). The accessibility of loop_{3–4} to the periplasm was confirmed by labeling with biotin maleimide; however, none of the Cys residues of loop_{1–2} were labeled by the reagent. These results suggest that the environments of the two loops are different (20).

In the present study, we analyzed PomA mutants with Cys substitutions in loop_{3–4}. A cross-linked form of these Cys-PomA proteins was detected under non-reducing conditions. We think that the cross-linked form is a homodimer and that the loops of PomA subunits are adjacent in the motor. We discuss the function and the structural topology of loop_{3–4} of PomA.

* This work was supported in part by grants-in-aid for scientific research from the Ministry of Education, Science and Culture of Japan (to M. H. and K. S.) and from the Japan Society for the Promotion of Science (to Y. A. and T. Y.). The costs of publication of this article were defrayed in part by the payment of page charges. This article must therefore be hereby marked "advertisement" in accordance with 18 U.S.C. Section 1734 solely to indicate this fact.

‡ To whom correspondence should be addressed. Tel.: 81-52-789-2991; Fax: 81-52-789-3001; E-mail: g44416a@nucc.cc.nagoya-u.ac.jp.

¹ The abbreviations used are: NEM, *N*-ethylmaleimide; DTT, dithiothreitol; PAGE, polyacrylamide gel electrophoresis.

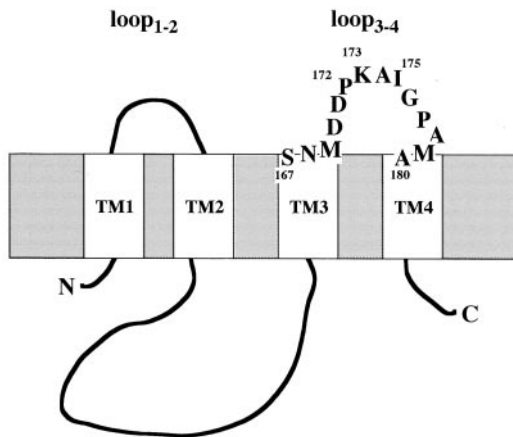


FIG. 1. Putative secondary structure of PomA. This secondary structure is based on the hydrophobic profiles (8) and the reactivity of Cys-substituted proteins with SH-modifying reagents (16). PomA has two putative periplasmic loops, loop₁₋₂ and loop₃₋₄. The amino acids in loop₃₋₄ are shown explicitly. The putative transmembrane (TM) regions are depicted as rectangles. Numbers indicate residue positions within PomA.

MATERIALS AND METHODS

Bacterial Strains, Plasmids, Growth Conditions, and Media—*V. alginolyticus* strains VIO5 (Rif^r, Pof⁺, Laf⁻), VIO586 (Rif^r, Pof⁺, Laf⁻, pomA), and NMB188 (Rif^r, Pof⁺, Laf⁻, Che⁻, pomA) were used (8, 11). *E. coli* strain DH5^λ (F⁻λ recA1 hsdR17 endA1 supE44 thi-1 relA1 gyrA96 Δ(argF-lacZYA) U169 φ80dlacZΔM15) was used for DNA manipulations. *V. alginolyticus* cells were cultured at 30 °C in VC medium: (0.5% (w/v) polypeptone, 0.5% (w/v) yeast extract, 0.4% (w/v) K₂HPO₄, 3% (w/v) NaCl, 0.2% (w/v) glucose); or VPG medium: (1% (w/v) polypeptone, 0.4% (w/v) K₂HPO₄, 3% (w/v) NaCl, 0.5% (w/v) glycerol). *E. coli* cells were cultured at 37 °C in LB medium. When necessary, kanamycin was added to a final concentration of 100 μg/ml for *V. alginolyticus* cells or 50 μg/ml for *E. coli* cells. Plasmid pYA301, a pSU41-based plasmid, carries the pomA gene under the control of the lac promoter (17).

Site-directed Mutagenesis—To introduce the P172A, P172I, and P172S substitutions into PomA, we used a two-step polymerase chain reaction method described previously (17). We synthesized pairs of mutant primers homologous to either the sense or antisense strand of the pomA gene, with a 1–3-base mismatch at the mutation site. In addition to these primers, we used end primers and amplified the full gene. This fragment was cloned into pSU41, and the identity of the total insert was confirmed by DNA sequencing.

Swarm Assay—An overnight culture in VC medium was spotted onto VPG plates containing 0.25% agar and 100 μg/ml kanamycin and incubated at 30 °C. Dithiothreitol (DTT) was added to a final concentration of 1 mM, as needed.

Measurement of Swimming Speed—Cells were harvested at late logarithmic phase and suspended in V-buffer (25 mM Tris-HCl, pH 7.5, 10 mM MgCl₂, 300 mM NaCl). The cell suspension was diluted 100-fold in V-buffer, and motility of the cells were observed at room temperature under a dark field microscope and recorded on video tape. Swimming speed was determined as described previously (25). If necessary, DTT was added to V-buffer at a final concentration of 1 mM.

Detection of Cys-PomA—VIO586 (PomA⁻) cells producing wild-type or various Cys-PomA mutant proteins were cultured in VPG medium and collected by centrifugation at mid-log phase. Cells were washed with V-buffer and then resuspended in the same buffer or in V-buffer containing 10 mM DTT or 1 mM CuCl₂. After 30 min of incubation at room temperature, the cells were collected, washed with V-buffer containing 2 mM N-ethylmaleimide (NEM), suspended in the same buffer, and then incubated at room temperature for 10 min. Next, an equal volume of 15% (w/v) trichloroacetic acid was added to the cell suspension, and the resulting precipitate was washed once with acetone, dried, and then dissolved in SDS sample buffer without reducing reagent. This sample was subjected to 12% SDS-polyacrylamide gel electrophoresis (SDS-PAGE) followed by immunoblotting with antibody against PomA, as described previously (18).

¹⁴C]NEM Modification—VIO586 cells producing wild-type or P172C PomA were grown in VPG medium to mid-log phase. The culture (80 ml) was centrifuged, and the cells were washed and suspended in V-buffer to an optical density at 660 nm of 10. After the cells were sonicated, the

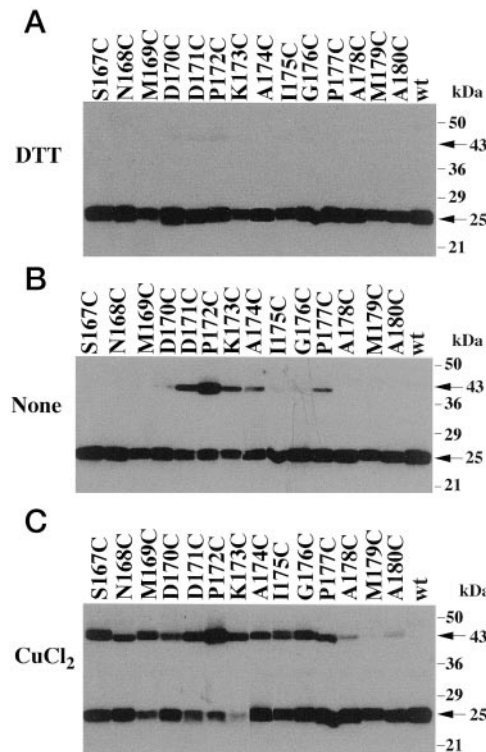


FIG. 2. Detection of Cys mutant PomA proteins. VIO586 (pomA⁻) cells harboring pYA301 (pomA⁺) and mutant derivatives were incubated in V-buffer (B) and buffer containing 10 mM DTT (A) or 1 mM CuCl₂ (C). After the cells were treated with 2 mM NEM, proteins were precipitated by trichloroacetic acid, washed with acetone, and separated by SDS-PAGE without reducing reagent. PomA was detected by immunoblotting with anti-PomA antibody. The PomA residues substituted with Cys are indicated. Numbers with arrows on the right side are the estimated molecular masses of the indicated bands.

cell debris was removed by centrifugation at 10,000 × g for 10 min at 4 °C, and the supernatant was then centrifuged at 100,000 × g for 60 min at 4 °C. The resulting precipitate (membrane fraction) was resuspended in V-buffer containing 10 mM DTT, and this suspension was incubated at room temperature. After 30 min, it was centrifuged at 100,000 × g for 60 min at 4 °C, the precipitate was resuspended in 500 μl of V-buffer containing 0.5 mM [¹⁴C]NEM (20 μCi/ml; NEN Life Science Products), and the resuspended material was incubated for 60 min at room temperature. The membrane fraction was recovered by centrifugation at 100,000 × g, solubilized with TNET buffer (50 mM Tris-HCl, pH 7.8, 150 mM NaCl, 5 mM EDTA, and 1% (w/v) Triton X-100), and incubated for 60 min at 4 °C. Immunoprecipitation with anti-PomA antibody was carried out as described previously (18). The resulting precipitates were subjected to SDS-PAGE, followed by fluorography.

RESULTS

Detection of Cys-PomA Protein—Asai *et al.* (20) carried out Cys-scanning mutagenesis of the two periplasmic loops (loop₁₋₂ and loop₃₋₄) of PomA and characterized the mutant proteins. This work showed that Cys replacements in loop₃₋₄ affected motility more severely than those in loop₁₋₂, and we therefore focused on the replacements in loop₃₋₄. When we examined Cys-PomA proteins in loop₃₋₄ by immunoblotting in the absence of reducing reagent, we observed, in addition to the 25-kDa PomA band, a 43-kDa band with Cys replacements at residues 171–174 and at residue 177 (Fig. 2B). The intensity of the 43-kDa band was greatest with the P172C protein. When cells were treated with DTT and immunoblotting was carried out, only the 25-kDa PomA band was observed (Fig. 2A). When the cells were treated with CuCl₂, the intensity of the 43-kDa band was greatly enhanced with the Cys mutant proteins, and the intensity of the 25-kDa PomA band was correspondingly

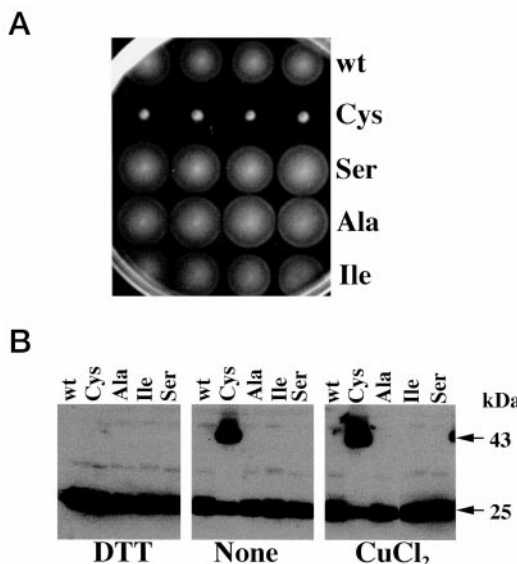


FIG. 3. Mutants with residue substitutions at PomA Pro-172. *A*, swarming abilities conferred by the mutant PomA proteins. Overnight cultures of VIO586 cells producing wild-type PomA (*wt*) and PomA P172C, P172S, or P172A were spotted onto 0.25% agar VPG plates containing 100 μ g/ml kanamycin and incubated at 30 °C for 3.5 h. *B*, immunoblotting of mutant PomA proteins. VIO586 cells producing PomA as in *A* were treated and immunoblotted as described in the legend to Fig. 2.

reduced (Fig. 2C). The 43-kDa band was never observed with wild-type PomA, which contains no cysteine residues.

To examine whether the 43-kDa band results from the Cys substitution and to test whether formation of the 43-kDa protein affects motor function, we constructed three additional Pro-172 mutants, P172A, P172I, and P172S. The motility of a *pomA* null mutant expressing any of these three PomA proteins was the same as that seen with wild-type PomA (Fig. 3A). In all three mutants, the 43-kDa band observed with P172C PomA was absent under all conditions tested (Fig. 3B).

Effect of DTT on Motility—Motility was more affected by Cys substitutions near residue Pro-172 than at other positions in the loop regions (20). The P172C mutant produced swarms only after prolonged incubation, and motile cells were seldom observed in liquid culture (data not shown). We predicted that the inhibition of motility is caused by disulfide-bound formation between PomA subunits. The residual motility is probably due to incomplete cross-linking (see below).

To examine this possibility, motility was assessed on swarm plates in the presence or absence of DTT (Fig. 4A). DTT did not affect swarming of cells expressing wild-type PomA, but cells producing P172C PomA swarmed well only in the presence of DTT (Fig. 4A). This result suggests that motility is restored by reductive cleavage of the disulfide cross-link between Cys-PomA molecules. We next tested for dominant-negative effects of the cross-linked form of PomA. When P172C PomA was produced in wild-type cells (VIO5) on agar plates without DTT, motility was significantly reduced (Fig. 4B). However, motility was restored in the presence of DTT. These results suggest that the cross-linked forms can be assembled into the motor complex.

To examine the relationship between recovery of motility and reduction of the cross-linked PomA further, we measured the swimming speed of cells in the presence of DTT and the amount of the cross-linked PomA in the cells (Fig. 5). The swimming speed of the cells with wild-type PomA did not change in the presence or absence of DTT, showing a result consistent with the swarming assay. The cells producing PomA P172C did not

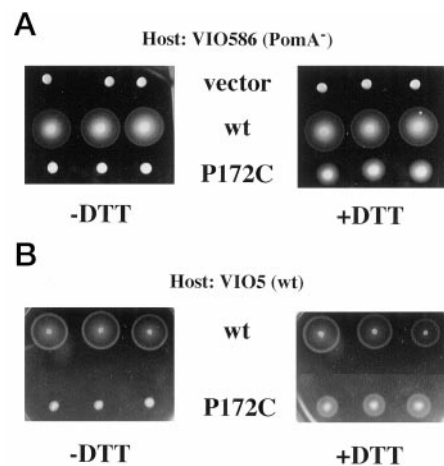


FIG. 4. Effect of DTT on motility. *A*, overnight cultures of VIO586 cells without PomA (vector) or producing wild-type PomA (*wt*) or PomA P172C were spotted onto 0.25% agar VPG plates containing 100 μ g/ml kanamycin in the absence (left) or the presence of 1 mM DTT (right) and incubated at 30 °C for 3.5 h. *B*, overnight cultures of wild-type VIO5 cells producing plasmid-encoded wild-type PomA (*wt*) or P172C PomA were spotted onto 0.25% agar VPG plates containing 100 μ g/ml kanamycin, as in *A*.

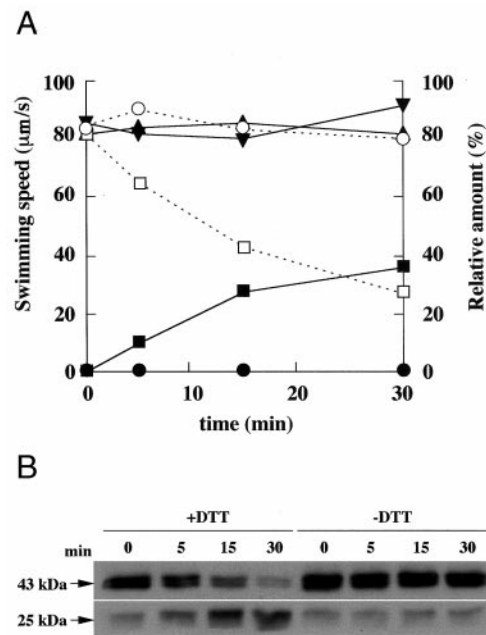


FIG. 5. Recovery of motility and reduction of the cross-linked PomA. *A*, swimming speed was measured in the presence or absence of 1 mM DTT as indicated under "Materials and Methods." Each filled symbol indicates swimming speeds of cells (strain NMB188) producing wild-type PomA in the presence (triangles) or absence (inverted triangles) of DTT, or PomA P172C in the presence (squares) or absence (circles) of DTT. Open symbols connected by dotted lines indicate relative amounts of 43-kDa PomA P172C dimer to total PomA P172C protein in the presence (squares) or absence (circles) of DTT. The amounts were estimated from the data shown in *B*. *B*, cells of strain NMB188 producing PomA P172C were collected at late logarithmic phase and suspended in V-buffer in the presence (left) or absence (right) of DTT. At the times indicated, cells were collected, and PomA was detected as described in the legend to Fig. 2.

swim in the absence of DTT. On the other hand, in the presence of DTT, the swimming speed of the cells gradually increased with time. After 30 min, the swimming speed of the cells producing PomA P172C recovered to about 40% compared with that of the cells with wild-type PomA (Fig. 5A). We observed a concomitant decrease in the amount of cross-linked PomA and an increase in the amount of monomeric PomA protein with

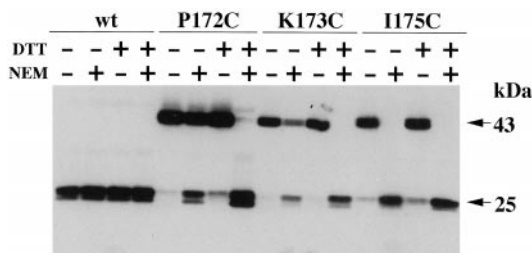


FIG. 6. Formation of cross-links. Cells producing wild-type PomA (*wt*) or PomA P172C, K173C, or I175C were incubated in V-buffer with or without 10 mM DTT, then incubated in buffer with or without 2 mM NEM, and finally incubated in buffer with 1 mM CuCl₂. PomA separated by SDS-PAGE was detected as described in the legend to Fig. 2. The symbols + or - above the lanes indicate incubation with or without DTT or NEM. Numbers on the right side are the estimated molecular masses corresponding to the bands indicated.

time. Immediately after DTT was added, the amount of the cross-linked PomA relative to total PomA in the cell was estimated to be about 80%. However, after 30 min in the presence of DTT, the amount of the cross-linked PomA decreased to only 25% of the total. Thus, the defect in motor function correlated with the amount of cross-linked PomA in the cell.

Extent of Cross-linking of the Cys Mutant PomA in Whole Cells—We sought to eliminate the possibility that cross-linking occurs during the isolation of proteins after cell lysis. NEM, which is a thiol group-specific reagent whose reaction is irreversible, was used to quench disulfide bond formation. Cells producing Cys-PomA were treated with DTT, then with NEM, and finally with CuCl₂, and immunoblotting was carried out with anti-PomA antibody (Fig. 6). Without DTT treatment, a decrease of the 43-kDa band in the P172C and K173C mutants was observed after the addition of NEM, and the band disappeared completely in the I175C mutant. When the cells were treated with both DTT and NEM, the 43-kDa band was significantly reduced in the P172C mutant and disappeared completely in the other two mutants. These results suggest that the disulfide bond is cleaved with DTT and that the cleaved Cys residue is modified with NEM, so that formation of the 43-kDa band upon oxidation with CuCl₂ is inhibited.

To examine whether P172C PomA is modified directly by NEM, the membrane fraction of cells producing either wild-type or mutant PomA was prepared and treated with DTT followed by [¹⁴C]NEM treatment. Labeled 25-kDa PomA, immunoprecipitated with anti-PomA antibody, was detected with the P172C mutant but not with the wild type (data not shown). This finding demonstrates that NEM directly modifies the thiol group of Cys in the P172C PomA protein.

Cross-linking of Cys-PomA Monomer—We wanted to establish that the 43-kDa protein is a cross-linked product of two Cys-PomA molecules and not PomA cross-linked to another protein. Membrane fractions were prepared from cells producing wild-type or P172C PomA and lysed with 1% (w/v) Triton X-100. Proteins were immunoprecipitated with anti-PomA antibody, and the precipitated proteins were separated by SDS-PAGE carried out with or without DTT and stained with Coomassie Brilliant Blue (Fig. 7). In the absence of DTT, the 25-kDa band or the 43-kDa band was detected with wild-type or P172C PomA, respectively. These bands were not detected in a control in which PomA was not produced although an unknown band above the 43-kDa band was detected. In the presence of DTT, only the 25-kDa form was detected with either wild-type or P172C PomA and the intensities of the bands were similar to the corresponding bands in the absence of DTT. In all lanes in the presence of DTT, the bands with a molecular mass of about 50 kDa are the heavy chains of IgG. These results

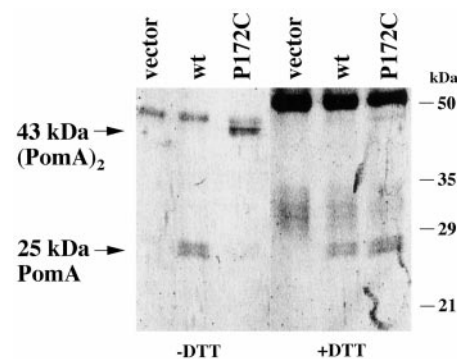


FIG. 7. Protein composition of the 43-kDa band. Membrane fractions prepared from VIO586 cells producing wild-type (*wt*) or P172C PomA were solubilized with 1% (w/v) Triton X-100, and immunoprecipitation was carried out with anti-PomA antibody. The precipitated proteins were separated by SDS-PAGE in the absence (left) or presence (right) of 10 mM DTT and stained with Coomassie Brilliant Blue. The antibody proteins were also stained by Coomassie Brilliant Blue in the gels. The numbers on the right side correspond to the positions of molecular size markers.

suggest that the 43-kDa band is composed entirely of cross-linked dimers between two Cys-PomA molecules.

DISCUSSION

The PomA protein of the Na⁺-driven flagellar motor of *Vibrio alginolyticus* is predicted to have four transmembrane segments, whereas the PomB, MotX, and MotY proteins have only a single transmembrane segment (8–11). From the predicted topology of PomA, the N- and C-terminal regions and the large loop between transmembrane segments 2 and 3 are located in the cytoplasm. Loop_{1–2} and loop_{3–4}, between transmembrane segments 1 and 2 and segments 3 and 4, respectively, are thought to be exposed to the periplasmic space (8). When the loops were reacted with biotin maleimide, the labeling pattern was different; substitutions in loop_{3–4} were biotinylated consistently with the membrane topology, whereas none of residues in loop_{1–2} was labeled (20). It has been proposed that loop_{1–2} is associated with other proteins, such as the motor proteins PomB, MotX, or MotY, or that it is embedded into the pore region of the channel, as is predicted for the extracellular loops of many ion channels. It has been shown that the negative charge Asp-31 of loop_{1–2} contributes to optimal speed and/or efficiency of the motor, although the charge is not essential (26). By random mutagenesis of the *pomA* gene, it was shown that loop_{3–4} and transmembrane segments 3 and 4 have residues more crucial for function than loop_{1–2} or transmembrane segments 1 and 2 (27).

In the present study, we focused on periplasmic loop_{3–4}. We found that the P172C mutant protein of PomA is not functional and inhibits the motility of the wild-type cell in the absence of reducing reagents, although motility is restored by DTT. This result suggests that a cross-link formed between two molecules of Cys-PomA via loop_{3–4} inhibits the function of the torque-generating units. The interaction between cross-linked PomA dimer and PomB is apparently not disrupted, since PomB appears to be co-precipitated about as well with the cross-linked PomA dimer as with the wild-type PomA (data not shown). It is inferred that two molecules of native PomA interact with each other intimately in a torque-generating unit of the motor. Recently, PomA alone was purified as a stable homodimer even if PomB was absent (19). The purified PomA/PomB complex has been reconstituted into proteoliposomes and has been shown to catalyze Na⁺ influx. Furthermore, a tandem PomA dimer produced as a single polypeptide is functional. Inactivation of either half of the dimer results in complete loss of PomA func-

tion. When a phenamil-resistant mutation was introduced into either the first or second half of the tandem PomA dimer, the resistant phenotype was identical to the phenotype of the tandem dimer in which the both halves carried the mutation. Thus, the two halves of the PomA dimer appear to function together (28).

The H⁺-driven flagellar motor contains MotA and MotB, which are homologues to PomA and PomB, respectively. It is thought that the MotA/MotB complex converts H⁺ influx into the rotation of the flagellar motor (4, 6, 29). From the results of Trp-scanning mutagenesis, a structural model of MotA/MotB complex has been proposed in which a single transmembrane segment of one MotB protein assembles with four transmembrane segments of one MotA protein at a tilt relative to them (5). If this model holds for the H⁺-driven motor, the existence of a heteromultimeric ion channel complex might be specific for the Na⁺-driven flagellar motor. On the other hand, estimates of the MotA and MotB protein levels in the membrane of *E. coli* suggest that the ratio of MotA to MotB is about 4:1 (30). This finding is consistent with the possibility that MotA and MotB do not make 1:1 complex.

The MotA protein of the H⁺-driven flagellar motor of *Rhodobacter sphaeroides* can generate torque in response to a sodium-ion flux in a *pomA* mutant of *V. alginolyticus* (31). MotA of *R. sphaeroides* may work in the Na⁺-driven motor because the torque generators in the H⁺- and Na⁺-driven motors have similar structures, *i.e.* they are heteromultimer complexes. In any case, clarification of the structure of the torque generator is clearly important for an understanding of the mechanism of coupling ion flow to flagellar rotation.

Two additional components, MotX and MotY, are required for the rotation of the Na⁺-driven motor of *V. alginolyticus*, but homologous proteins are not found in the H⁺-driven motor (9–12). The functions of MotX and MotY are not clear, although it is thought that they may be involved in ion recognition. MotX and MotY do not co-purify with the PomA/PomB complex (19). This observation may mean that MotX and MotY are not associated with the PomA/PomB complex, that the association is weak, or that MotX and MotY are unstable during purification. It will be interesting to determine the structural difference between the torque generators of the Na⁺- and H⁺-driven flagellar motors.

It has been proposed that the rotor is surrounded with multiple torque-generating units, approximately eight units in the H⁺-driven flagellar motor (32) or five to nine in the Na⁺-driven motor (33). We can envision two models to explain the cross-linking of PomA molecules. One is an intra-torque-generator model, in which the cross-links form between two PomA molecules in the same unit. In this argument, loop_{3–4} must face into the unit. The other possibility is an inter-torque-generator model, in which the cross-link occurs between two PomA molecules in different units, so that the loop_{3–4} faces outward. The former model is supported by following criteria; the distance between two generators may be too great for disulfide cross-link to form, PomA forms a stable dimer in the cell, and genetically connected tandem PomA is functional. We need more experiments to elucidate which model is correct.

Residue Pro-172 by itself does not seem to be essential for motor function, since motility is normal in PomA mutants in which Pro-172 was replaced by three amino acids other than Cys. Additionally, we observed recovery of swimming ability when the cross-linked dimer was reduced in cells with P172C PomA by DTT. We suggest that the flexibility of loop_{3–4} is restricted by the cross-linking, thereby impairing motor function. There are at least three possible mechanisms for this inhibition of motor function. (i) Na⁺ influx is inhibited by disruption of the channel structure. (ii) Conversion of the Na⁺ influx to conformational changes in the torque-generating stator units is inhibited. (iii) Interactions between the stator and the rotor are inhibited. Understanding of the inhibitory mechanism might lead us to an understanding of the energy transduction mechanism in the flagellar motor.

Acknowledgment—We thank R. M. Macnab for critically reading the manuscript.

REFERENCES

1. Aizawa, S. I. (1996) *Mol. Microbiol.* **19**, 1–5
2. Imae, Y., and Atsumi, T. (1989) *J. Bioenerg. Biomembr.* **21**, 705–716
3. Manson, M. D., Tedesco, P., Berg, H. C., Harold, F. M., and van der Drift, C. (1977) *Proc. Natl. Acad. Sci. U. S. A.* **74**, 3060–3064
4. Blair, D. F., and Berg, H. C. (1990) *Cell* **60**, 439–449
5. Sharp, L. L., Zhou, J. D., and Blair, D. F. (1995) *Biochemistry* **34**, 9166–9171
6. Stolz, B., and Berg, H. C. (1991) *J. Bacteriol.* **173**, 7033–7037
7. Tang, H., Braun, T. F., and Blair, D. F. (1996) *J. Mol. Biol.* **261**, 209–221
8. Asai, Y., Kojima, S., Kato, H., Nishioka, N., Kawagishi, I., and Homma, M. (1997) *J. Bacteriol.* **179**, 5104–5110
9. McCarter, L. L. (1994) *J. Bacteriol.* **176**, 4219–4225
10. McCarter, L. L. (1994) *J. Bacteriol.* **176**, 5988–5998
11. Okunishi, I., Kawagishi, I., and Homma, M. (1996) *J. Bacteriol.* **178**, 2409–2415
12. Furuno, M., Nishioka, N., Kawagishi, I., and Homma, M. (1999) *Microbiol. Immunol.* **43**, 39–43
13. Hase, C. C., and Mekalanos, J. J. (1999) *Proc. Natl. Acad. Sci. U. S. A.* **96**, 3183–3187
14. Jaques, S., Kim, Y. K., and McCarter, L. L. (1999) *Proc. Natl. Acad. Sci. U. S. A.* **96**, 5740–5745
15. Kojima, S., Yamamoto, K., Kawagishi, I., and Homma, M. (1999) *J. Bacteriol.* **181**, 1927–1930
16. Kojima, S., Atsumi, T., Muramoto, K., Kudo, S., Kawagishi, I., and Homma, M. (1997) *J. Mol. Biol.* **265**, 310–318
17. Kojima, S., Asai, Y., Atsumi, T., Kawagishi, I., and Homma, M. (1999) *J. Mol. Biol.* **285**, 1537–1547
18. Yorimitsu, T., Sato, K., Asai, Y., Kawagishi, I., and Homma, M. (1999) *J. Bacteriol.* **181**, 5103–5106
19. Sato, K., and Homma, M. (2000) *J. Biol. Chem.* **275**, 5718–5722
20. Asai, Y., Shoji, T., Kawagishi, I., and Homma, M. (2000) *J. Bacteriol.* **182**, 1001–1007
21. Frillingos, S., Sahin, T. M., Wu, J., and Kaback, H. R. (1998) *FASEB J.* **12**, 1281–1299
22. Kimura, T., Nakatani, M., Kawabe, T., and Yamaguchi, A. (1998) *Biochemistry* **37**, 5475–5480
23. Kubo, Y., Yoshimichi, M., and Heinemann, S. H. (1998) *FEBS Lett.* **435**, 69–73
24. Perez-Garcia, M. T., Chiamvimonvat, N., Marban, E., and Tomaselli, G. F. (1996) *Proc. Natl. Acad. Sci. U. S. A.* **93**, 300–304
25. Homma, M., Oota, H., Kojima, S., Kawagishi, I., and Imae, Y. (1996) *Microbiology* **142**, 2777–2783
26. Kojima, S., Shoji, T., Asai, Y., Kawagishi, I., and Homma, M. (2000) *J. Bacteriol.* **182**, 3314–3348
27. Kojima, S., Kuroda, M., Kawagishi, I., and Homma, M. (1999) *Microbiology* **145**, 1759–1767
28. Sato, K., and Homma, M. (2000) *J. Biol. Chem.* **275**, 20223–20228
29. Blair, D. F. (1995) *Annu. Rev. Microbiol.* **49**, 489–522
30. Wilson, M. L., and Macnab, R. M. (1990) *J. Bacteriol.* **172**, 3932–3939
31. Asai, Y., Kawagishi, I., Sockett, R. E., and Homma, M. (1999) *J. Bacteriol.* **181**, 6332–6328
32. Blair, D. F., and Berg, H. C. (1988) *Science* **242**, 1678–1681
33. Muramoto, K., Sugiyama, S., Cragoe, E. J., Jr., and Imae, Y. (1994) *J. Biol. Chem.* **269**, 3374–3380